Journal of Molecular Structure 1216 (2020) 128330

Contents lists available at ScienceDirect

Journal of Molecular Structure

journal homepage: http://www.elsevier.com/locate/molstruc

Efficient separation of perrhenate as analogue to pertechnetate in nitric acid solution with a DOTA-tetraamide ligand: Solvent extraction, complexation and structure study

Xueyu Wang [1], Xiaoyang Hu [1], Lianjun Song , Xiuying Yang , Qian Xiao , Haowei Xu , Songdong Ding [*]

College of Chemistry, Sichuan University, Chengdu, 610064, PR China

ARTICLE INFO

Article history:
Received 30 January 2020
Received in revised form
16 April 2020
Accepted 23 April 2020
Available online 28 April 2020

Keywords:
Cyclen
DOTA-Tetraamide
Pertechnetate
Perrhenate
Solvent extraction
Complexation

ABSTRACT

The two DOTA-tetraamide ligands, DOTAM-*n*-butyl (1,4,7,10-tetrakis[(*N*-*n*-butyl; carbamoyl)methyl]-1,4,7,10-tetraazacyclododecane) and DOTAM-benzyl (1,4,7,10- tetrakis[(*N*-benzylcarbamoyl)methyl]-1,4,7,10-tetraazacyclododecane), were synthesized and characterized by MS, NMR and FTIR spectra. In acid solution, DOTAM-*n*-butyl was liable to be protonated. FTIR, ^{1}H NMR, ESI-MS spectra and X-ray diffraction analyses revealed that the nitrogen atoms of cyclen ring combined two protons to form a cation with two positive charges. The protonated DOTAM-*n*-butyl had strong extraction ability and good selectivity for ReO_4^-. It was extracted by means of the substitution of one ReO_4^- for one NO_3^- in the 1:2 complex of DOTAM-*n*-butyl with HNO_3. The solvent extraction and X-ray crystallography demonstrated an anion-exchange extraction model. Meanwhile, X-ray crystal structure analyses of ligand complexes with $HReO_4$ or HNO_3 also indicated that ReO_4^- or NO_3^- ions were located in the gap between the upper and lower protonated ligands through multiple hydrogen bonds and electrostatic interactions.

1. Introduction

Over the past few decades, about 400 metric tonnes of technetium-99 (^{99}Tc) have been produced during the nuclear fission of ^{235}U or ^{239}Pu [1,2]. ^{99}Tc as a β-emitter with a long half-life of 2.13×10^5 years is one of the most problematic radionuclides in acidic nuclear waste [3–5], and primarily exists in the +7 oxidation state as TcO_4^- in both the nuclear fuel cycle and environments under oxic conditions [6,7]. However, due to large water solubility (11.3 mol/L for the sodium salt at 20 °C) and extremely high mobility in the environment, TcO_4^- has a real threat to environmental and public health [6,8]. Additionally, during the nuclear waste vitrification process, high volatility of technetium would also lead to the generation of volatile technetium compounds such as Tc_2O_7, which is not good for its ultimate disposal [9]. Thus, in order to mitigate long-term nuclear waste storage issues, it is very essential to removal of radioactive pertechnetate from acidic nuclear waste.

Generally, liquid-liquid solvent extraction is one of the most commonly used separation methods in experiment and engineering for reprocessing of spent nuclear fuel [10–14]. Up to now, some extractants for separating TcO_4^- have been developed such as tertiary amine TOA and quaternary amine Aliquat-336 [15–18]. Through electrostatic interaction between TcO_4^- and positively charged extractant, technetium as a hydrophobic ion pair is extracted from aqueous phase into organic phase. These extractants have good extraction performances for TcO_4^-. However, they suffered from very low extraction capacity, resulting in the frequent appearance of the second organic phase or emulsification [18,19]. This greatly hampers their applications in practical process. Therefore, it is significant to explore the new and efficient extractant for TcO_4^- separation.

In recent years, it was found that macrocyclic polyamine receptors had an excellent selective recognition and trapping of pertechnetate in aqueous solution [20–22]. For example, the *p*-xylyl aza-cryptand receptor consists of a macro-bicyclic polyamine which is made of two bis-tren units linked by *p*-xylyl spacers. Owing to the stabilization of the inclusion complex by multiple

* Corresponding author.
E-mail address: dsd68@163.com (S. Ding).
[1] These authors contributed equally to this work.

https://doi.org/10.1016/j.molstruc.2020.128330
0022-2860/

strong H-bonding interactions with the protonated imino groups in the cavity, there is so very high affinity for TcO_4^- that the affinity constant is about two and three orders of magnitude higher than for ClO_4^- and NO_3^-, respectively [23]. After the introduction of a fluorescent unit such as anthracenyl group in the aza-cryptand's framework, the receptor was able to selectively recognize and sense TcO_4^- at μmol/L concentration [24]. Consequently, there are good reasons to expect that an efficient TcO_4^- separation may be achieved in the event that this kind of water-soluble macrocyclic polyamine receptor is modified as a lipid-soluble extractant. One of the effective modification methods is to reduce the number of imino groups to suppress the formation of highly protonated species with pronounced hydrophilicity. In other words, this also means to reduce the ring size of macrocyclic polyamine. Among the macrocyclic polyamines with smaller ring, 1,4,7,10-tetrazacyclododecane, "cyclen", is the most representative one. Its tetraamide derivatives (Fig. 1) have eight donor atoms, i.e. four N atoms of cyclen ring and four carbonyl O atoms of four side arms. There is the cooperativity between cyclen ring and cyclen-side arms, producing an expanded cavity. So these ligands can effectively extract and encapsulate metal ion with different ionic radius, such as Na^+, Pd^{2+}, Eu^{3+} and Gd^{3+} [25–29]. For example, Tsukube et al. investigated the extraction behaviors of Li^+, Na^+ and K^+ ions by amide-armed cyclen L_1 (Fig. 1) in CH_2Cl_2 [25,26]. The extraction percentage of Na^+ was recorded up to 86%, whilst that of Li^+ or K^+ was less than 10% under the same conditions, showing good selectivity for Na^+. Xia et al. also reported a similar armed cyclen L_2 (Fig. 1) and its extraction behaviors toward some actinide cations in HNO_3 solution using CH_2Cl_2 as diluent [30]. The ligand L_2 exhibited excellent selectivity for Th^{4+}. At pH > 4.2, about 90% Th^{4+} was extracted into organic phase. Furthermore, due to four N atoms on the ring, the cyclen-based ligands have complicated protonization behavior. Multistep protonations commonly take place on the amine groups of cyclen ring [27,28]. In theory, these protonations may be good for the extraction of negative ions via electrostatic attraction. But unfortunately there have so far been no reports on the extraction of anions such as TcO_4^- by DOTA-tetraamides.

It is well known that Tc is a radioactive nuclide and difficult to be obtained, but Re, which lies below Tc in the periodic table, has stable isotopes and its oxometallate ReO_4^- is sufficiently similar to TcO_4^-. They have similar ionic radii (TcO_4^- = 2.52 Å and ReO_4^- = 2.60 Å) and metal oxygen bond lengths (Tc—O = 1.702 Å and Re—O = 1.719 Å) [4,22]. Consequently, ReO_4^- can be often used as an analogue for TcO_4^- in solvent extraction [31]. In the present paper, the ligands DOTAM-*n*-butyl and DOTAM-benzyl (Scheme 1) were synthesized, and by employing ReO_4^- as a surrogate for TcO_4^-, the extraction behaviors of DOTAM-*n*-butyl toward ReO_4^- in HNO_3 solution were investigated. And then, the complexation of DOTAM-*n*-butyl with ReO_4^-, as well as the complex structures were also studied by using ^{1}H NMR, FTIR, ESI-MS and single crystal X-ray diffraction. Moreover, the extraction model was presented too.

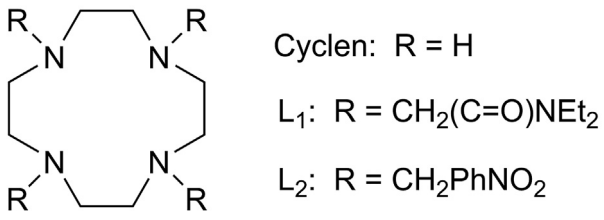

Fig. 1. Chemical structures of cyclen and its derivatives.

2. Experimental

2.1. Reagents

ReO_4^- in HNO_3 solution was prepared from NH_4ReO_4 (99.999%, Alfa Aesar). Cl^-, $H_2PO_4^-$ and SO_4^{2-} in HNO_3 solution were prepared from NaCl, NaH_2PO_4 and Na_2SO_4 (99.9%, Aladdin, China). And all the other reagents used in the experiments were of analytical grade without further purification unless otherwise stated.

FTIR spectra were recorded on a Nicolet Nexus 670 Model instrument. ^{1}H NMR spectra were measured on a Varian Inova 400 MHz NMR spectrometer using methanol-d4, chloroform-d or dimethyl sulfoxide-d6 as solvent with tetramethylsilane as internal standard. High resolution ESI-MS spectra were obtained on a LCMS-IT-TOF spectrometer. The pH of the aqueous phase was measured by an INESA PHS-3C pH meter equipped with an E−201-C pH glass electrode.

2.2. Synthesis

N-*n*-butyl bromoacetamide and *N*-benzyl bromoacetamide were prepared by previously published methods [32,33]. DOTAM-*n*-butyl and DOTAM-benzyl were synthesized according to Scheme 1.

Under a nitrogen atmosphere at room temperature, triethylamine (5.06 g, 50 mmol) was added to a solution of 1,4,7,10-tetraazacyclododecane (1.03 g, 6 mmol) and bromoacetamide (24 mmol) in 100 mL CH_3CN (for DOTAM-*n*-butyl) or THF (for DOTAM-benzyl). The reaction mixture was stirred at 65 °C for 2 days. After cooling, the white solid was filtered and washed with cold CH_3CN and ice-cold water, then dried under vacuum and recrystallized from CH_3CN to afford the title compound as a colorless solid.

DOTAM-n-butyl. (2.30 g, 61%) mp: 161–162 °C. FTIR (KBr, ν/cm^{-1}): 3464, 3294(NH), 3236 (NH), 3080, 2958, 2933, 2870, 2823, 1659(C=O), 1554, 1456, 1306, 1238, 1101, 715. ^{1}H NMR (400 MHz, CD_3OD, ppm): δ 3.21 (t, 8H, CH_2CH_2NH), 3.08 (s, 8H, NCH_2CO), 2.73 (s, 16H, ring NCH_2CH_2N), 1.57–1.44 (m, 8H, $CH_3CH_2CH_2$), 1.43–1.29 (m, 8H, $CH_3CH_2CH_2$), 0.95 (t, 12H, CH_3CH_2). ^{13}C NMR (100 MHz, CD_3OD, ppm): δ 173.7 (*C*O), 59.9 (NCH_2CO), 54.9 (ring NCH_2 CH_2N), 40.2 (CH_2CH_2NH), 33.0 ($CH_3CH_2CH_2$), 21.4 ($CH_3CH_2CH_2$), 14.3 ($CH_3CH_2CH_2$). ESI-MS (*m*/*z*): Found: 625.5083 ([M+H]$^+$), 647.4899 ([M+Na]$^+$). Calcd: 625.5123 ([M+H]$^+$), 647.4943 ([M+Na]$^+$).

DOTAM-benzyl. (2.40 g, 53%) FTIR (KBr, ν/cm^{-1}): 3305, 3203, 3059, 3030, 2945, 2818, 1651(C=O), 1552, 1456, 1365, 1306, 1257, 1103, 739, 700, 615. ^{1}H NMR (400 MHz, $CDCl_3$, ppm): δ 7.31–7.15 (m, 20H, Ar), 7.10 (t, J = 6.0 Hz, 4H, CONH), 4.29 (d, J = 5.8 Hz, 8H, $ArCH_2$), 2.90 (s, 8H, NCH_2CO), 2.45 (s, 16H, ring NCH_2CH_2N). ^{13}C NMR (100 MHz, $CDCl_3$, ppm): δ 138.4, 128.8, 127.8, 127.6, 59.0, 53.7, 43.0. ESI-MS (*m*/*z*): Found: 761.4493 ([M+H]$^+$), 783.4300 ([M+Na]$^+$). Calcd: 761.4502 ([M+H]$^+$), 783.4322 ([M+Na]$^+$).

HNO_3 Complex of DOTAM-n-butyl (*DOTAM-n-butyl-HNO_3*). A solution of DOTAM-*n*-butyl (0.13 g, 0.20 mmol) in CH_2Cl_2 (2 mL) was added to a 0.20 mol/L HNO_3 solution (2 mL), and the mixture was stirred at room temperature for 2 h. After centrifugation, the CH_2Cl_2 phase was removed and the water phase was subsequently concentrated under reduced pressure, and the white solid was obtained. Crystals suitable for X-ray diffraction were obtained by slow diffusion of ethyl acetate (EA) into the CH_3OH solution after 3 weeks. FTIR (KBr, ν/cm^{-1}): 3354, 3268, 3082, 2960, 2932, 2868, 1682(C=O), 1648(C=O), 1558, 1459, 1384(NO_3^-). ^{1}H NMR (400 MHz, DMSO-d_6, ppm): δ 8.20 (s, 4H, CONH), 7.83 (s, 2H, ring NH), 3.57 (s, 8H, NCH_2CO), 3.27–3.13 (d br, 16H, ring NCH_2CH_2N), 3.10–3.05 (q, 8H, CH_2CH_2NH), 1.44–1.37 (m, 8H, CH_2CH_2NH), 1.32–1.23 (m, 8H, $CH_3CH_2CH_2$), 0.87 (t, 12H, CH_3CH_2). ESI-MS (*m*/*z*): Found: 313.2558

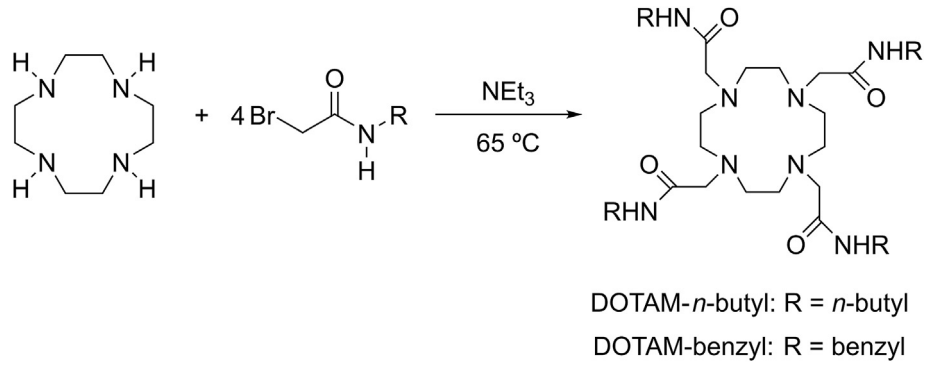

Scheme 1. Synthetic route of DOTAM-*n*-butyl and DOTAM-benzyl.

($[M+2H]^{2+}$). Calcd: 313.2603 ($[M+2H]^{2+}$).

$HReO_4$ Complex of DOTAM-n-butyl (*DOTAM-n-butyl-$HReO_4$*). A solution of DOTAM-*n*-butyl (0.13 g, 0.20 mmol) in CH_2Cl_2 (2 mL) was added to a 0.20 mol/L HNO_3 solution (2 mL) with NH_4ReO_4 (0.11 g, 0.40 mmol). The mixture was stirred at room temperature for 2 h. And the white solid was obtained by filtration. Single crystals were obtained by slow diffusion of EA into a solution in CH_3OH after 3 weeks. FTIR (KBr, ν/cm^{-1}): 3358, 3282, 3081, 2960, 2933, 2868, 1683(C═O), 1647(C═O), 1558, 1460, 1385, 917(ReO_4^-). ^{1}H NMR (400 MHz, DMSO-d_6, ppm): δ 8.18 (s, 4H, CON*H*), 7.83 (s, 2H, ring N*H*), 3.57 (s, 8H, NCH_2CO), 3.27–3.12 (d br, 16H, ring NCH_2CH_2N), 3.10–3.05 (q, 8H, CH_2CH_2NH), 1.44–1.37 (m, 8H, CH_2CH$_2$NH), 1.32–1.23 (m, 8H, CH$_3$CH_2CH$_2$), 0.87 (t, 12H, CH_3CH$_2$). ESI-MS (*m*/*z*): Found: 313.2586 ($[M+2H]^{2+}$). Calcd: 313.2603 ($[M+2H]^{2+}$).

$HReO_4$ Complex of DOTAM-benzyl (*DOTAM-benzyl-$HReO_4$*). DOTAM-benzyl (0.038 g, 0.05 mmol) in 30 mL mixed solution of CH_3CN/CH_3OH (v:v, 10:1) was added to 0.20 mol/L HNO_3 solution (1 mL) with NH_4ReO_4 (0.027 g, 0.10 mmol). The mixture was stirred at room temperature for 2 h. Then the solvents were removed in vacuo and the white solid was obtained. Crystals suitable for X-ray diffraction were obtained by slow evaporation of CH_3OH/H_2O solution after 2 weeks. FTIR (KBr, ν/cm^{-1}): 3439, 3340, 3062, 2844, 1684(C═O), 1647(C═O), 1558, 1454, 1387, 1262, 916(ReO_4^-), 731, 696. ^{1}H NMR (400 MHz, DMSO-d_6, ppm): δ 8.73 (s, 4H, CON*H*), 7.95 (s, 2H, ring N*H*), 7.21 (s br, 20H, Ar), 4.26 (d, J = 5.8 Hz, 8H, ArCH_2), 3.74 (s, 8H, NCH_2CO), 3.21 (s br, 16H, ring NCH_2CH_2N). ESI-MS (*m*/*z*): Found: 381.2290 ($[M+2H]^{2+}$). Calcd: 381.2290 ($[M+2H]^{2+}$).

2.3. Solvent extraction

Solvent extraction was performed by mixing the organic phase and the aqueous phase. The 2.7×10^{-4} mol/L ReO_4^- in HNO_3 solution, the mixed solution of anions with ReO_4^- or the pure HNO_3 solution was used as the aqueous phase. DOTAM-*n*-butyl dissolved in benzyl alcohol or other diluents were employed as the organic phase. Before the extraction of ReO_4^-, the organic phase was pre-equilibrated with the corresponding concentration of HNO_3 solution. During an investigation for the extraction of alone HNO_3, there was no need for this pre-equilibration step. Equal volumes (1.0 mL) of the organic phase and the aqueous phase were stirred in a 10 mL stoppered glass tube in water bath at 25.0 ± 0.5 °C for the desired time. After phase separation by centrifugation, the aqueous phase was taken out for analysis. The equilibrium concentrations of HNO_3 in aqueous phase were determined by acid-base titration or using pH meter (PHS–3C, Shanghai INESA, China). Those of ReO_4^- were measured by an inductively coupled plasma optical emission spectrometer (ICP-OES, Optima 8000, PerkinElmer). The anions such as Cl^-, $H_2PO_4^-$ and SO_4^{2-} were analyzed using ion chromatography (PIC-10, Qingdao Puren, China) equipped with a conductivity detector. Meanwhile, the concentrations of ReO_4^- and the other anions in organic phase were calculated from mass balances by the difference between initial solution and aqueous phase after extraction. All extraction experiments were carried out in triplicate.

The extraction efficiency of HNO_3 was gotten as follows:

$$E = \frac{[HNO_3]_{ini.} - [HNO_3]_{eq.}}{[HNO_3]_{ini.}} \times 100\% \quad (1)$$

where E, $[HNO_3]_{ini.}$ and $[HNO_3]_{eq.}$ represent extraction efficiency, initial concentration and equilibrium concentration of HNO_3 in the aqueous phase, respectively.

Besides, the distribution ratio (D) was obtained as the ratio of the total ion concentration in organic phase ($[M]_{org.}$) to that in aqueous phase ($[M]_{aq.}$).

$$D_M = \frac{[M]_{org.}}{[M]_{aq.}} \quad (2)$$

where the subscripts org. and aq. represent the organic phase and aqueous phase, separately. The separation factor (SF) of ReO_4^- toward the other ion was calculated by the formula:

$$SF_{Re/M} = \frac{D_{Re}}{D_M} \quad (3)$$

2.4. Single crystal X-ray diffraction analyses

Single crystal X-ray diffraction measurements were carried out using an Agilent Technologies Gemini diffractometer. Using *Olex2* [34], the structure was solved with the *ShelXT* [35] structure solution program using Direct Methods and refined with the *ShelXL* [36] refinement package using Least Squares minimization. All of the non-hydrogen atoms were refined anisotropically and the hydrogen atoms were refined by using riding coordinates. Hydrogens bonded to carbon and nitrogen were positioned in geometric positions and given thermal parameters equivalent to 1.2 times (or 1.5 times for methyl groups) those of the atoms to which they were bonded. Crystal data, details of the data collection and the structure refinement of complexes were given in Table S1. Crystallographic data for the single crystals reported in this work have been deposited with the Cambridge Crystallographic Data Centre as a supplementary publication, CCDC 1449197 (DOTAM-*n*-butyl), 1485999 (DOTAM-*n*-butyl-HNO_3), 1505095 (DOTAM-*n*-butyl-$HReO_4$) and 1506110 (DOTAM-benzyl-$HReO_4$). These data can be

obtained free of charge from The Cambridge Crystallographic Data Centre via www.ccdc.cam.ac.uk/data_request/cif.

3. Results and discussion

3.1. Solvent extraction

Prior screening tests had shown that both DOTAM-*n*-butyl and DOTAM-benzyl had poor solubility in the commonly used diluents such as kerosene and toluene. Especially for DOTAM-benzyl, there were few hydrophobic solvents to dissolve it. Consequently, its extraction behaviors were not examined. Nevertheless, for DOTAM-*n*-butyl, it is fortunate that it could be dissolved in benzyl alcohol, *n*-octanol and dichloromethane. Therefore, the influence of the diluent on the extraction of ReO_4^- by DOTAM-*n*-butyl was listed in Table S8. It was found that benzyl alcohol was the best fit for the extraction. Thus, in the following extraction experiments, benzyl alcohol was chosen as a diluent.

DOTAM-*n*-butyl is a basic amine ligand. In order to achieve extraction for ReO_4^-, it must initially be converted to an appropriate amine salt in the organic phase by reacting it with an acid in the medium. This reaction is known as "pre-equilibration" [37,38]. The results of pre-equilibration experiment were listed in Table 1. It was clear that the acidity of the aqueous phase did not change anymore after being equilibrated with 0.10 mol/L HNO_3 solution thrice, indicating a complete HNO_3 pre-equilibration. This means that the ligand was totally converted to its amine salt. Meanwhile, it can also be seen that approximate 0.17 mol/L HNO_3 were extracted into the organic phase of 0.10 mol/L DOTAM-*n*-butyl in benzyl alcohol, suggesting the possible formation of 1:2 ligand/HNO_3 extracted complexes. Hence, during the subsequent ReO_4^- extraction, three times pre-equilibrium with the corresponding concentration of HNO_3 solution was necessary.

The influence of contact time, acidity, NO_3^- concentration and ligand concentration on the extraction of ReO_4^- by DOTAM-*n*-butyl in benzyl alcohol were investigated with the results shown in Fig. 2. Fig. 2a displayed the influence of contact time on the extraction. Within about 40 min, the extraction equilibrium reached. To ensure the complete equilibrium, 60 min was chosen as two-phase contact time. The influence of HNO_3 concentration on the extraction was illustrated in Fig. 2b. The sole benzyl alcohol has very weak extraction ability toward ReO_4^- with D_{Re} value less than 1.0. Once DOTAM-*n*-butyl ligand was added into benzyl alcohol, D_{Re} value increased steeply, especially at low acidity, indicating that DOTAM-*n*-butyl can extract effectively ReO_4^-. With increasing HNO_3 concentration, D_{Re} value decreased, which could be attributed to the competition extraction of NO_3^-. Thus, the influence of NO_3^- concentration was also examined and showed in Fig. 2c. The plot of $\lg D_{Re}$ vs $\lg[NO_3^-]$ gave a straight line with a slope value close to -1, suggesting that one NO_3^- was involved in the extraction reaction. To determine the number of DOTAM-*n*-butyl molecules in the extraction reaction, slope analysis was also used on the basis of the influence of extractant concentration on the extraction shown in Fig. 2d. It was clear that D_{Re} values increased with the rise of DOTAM-*n*-butyl concentration. Meanwhile, the plot of $\lg D_{Re}$ vs $\lg$ [DOTAM-*n*-butyl] also gave a straight line with a slope value of 1.0, revealing the formation of 1:1 complex of DOTAM-*n*-butyl with ReO_4^-. Therefore, according to these results, it could be inferred that ReO_4^- was extracted by means of the substitution of one ReO_4^- for one NO_3^- in the 1:2 complex with HNO_3. The extraction equilibrium equation could be expressed as follows:

$$\left[H_2L^{2+}\cdot 2NO_3^-\right]_{org.} + {ReO_4^-}_{aq.} \rightleftharpoons \left[H_2L^{2+}\cdot NO_3^-\cdot ReO_4^-\right]_{org.} + {NO_3^-}_{aq.} \quad (4)$$

where L represents ligand and the subscripts org. and aq. denote the organic phase and aqueous phase, respectively.

The extraction of ReO_4^- in HNO_3 solution by DOTAM-*n*-butyl follows an anion-exchange extraction model. At first, the ligand was protonated in organic phase, resulting in the formation of 1:2 complex of the ligand with HNO_3, namely, H_2DOTAM-*n*-butyl$^{2+}\cdot 2NO_3^-$. And then one of the two NO_3^- ions was exchanged with ReO_4^- ion in aqueous phase, producing a more hydrophobic ion-pair of H_2DOTAM-*n*-butyl$^{2+}\cdot NO_3^-\cdot ReO_4^-$. As a result, ReO_4^- ions were extracted from aqueous phase to organic phase. The extraction process can described by Scheme 2.

Due to the electrostatic repulsion, the protonated DOTAM-*n*-butyl hardly extracted metal cations under acidic condition (Fig. S17). Nevertheless, the negatively-charged ions such Cl^-, $H_2PO_4^-$ and SO_4^{2-}, which commonly present in acidic nuclear waste, might have a big impact on the ReO_4^- extraction. And for this, the extraction selectivity of DOTAM-*n*-butyl for ReO_4^- was investigated. As shown in Table 2, the distribution ratios of ReO_4^- were significantly greater than those of the other anions of Cl^-, $H_2PO_4^-$ and SO_4^{2-}. It could be attributed to the following two main reasons. On one hand, the hydration ability of $H_2PO_4^-$ and SO_4^{2-} was much stronger than that of ReO_4^-. On other hand, Cl^- had the similar hydration energy to ReO_4^-, but its ionic radius was obviously less than that of ReO_4^-, meaning that the latter was more hydrophobic and easier extracted than the former. Meanwhile, the separation factors of ReO_4^- over the three anions could also reach the level of several tens, indicating a good selectivity for ReO_4^-. Moreover, under the same conditions, DOTAM-*n*-butyl had an obviously higher loading capacity of ReO_4^- than that of TOA or Aliquat-336 (Fig. S18). This is also good for the extraction separation of ReO_4^-.

Table 1
Equilibration experiment of 0.10 mol/L DOTAM-*n*-butyl in benzyl alcohol with equal volume of HNO_3 solution.

Organic phase	$[HNO_3]_{ini.}$, mol/L	$[HNO_3]_{eq.}$, mol/L	*E*, %
Initial	0.10	$< 1 \times 10^{-4}$	100
equilibrated once	0.10	0.035	65
equilibrated twice	0.10	0.091	9
equilibrated thrice	0.10	0.10	0

3.2. Complexation and structure of DOTAM-n-butyl with HNO_3 and ReO_4^-

Generally, study on the complexation of extracted ions with the extractant can not only help in obtaining information of the complex composition and structure, and also contribute to deeply understanding the extraction model. Thus, the complexation behavior of DOTAM-*n*-butyl with ReO_4^- was investigated using ^{1}H NMR and FTIR spectra analyses. The white solid complexes of DOTAM-*n*-butyl with both ReO_4^- and NO_3^- were obtained by means of solvent diffusion as described in the experimental section.

3.2.1. ^{1}H NMR spectra analysis

NMR spectroscopy is the most powerful mean for the identifications of structural groups, whose main feature is that the chemical shift measured by this technique is strongly dependent on the chemical environment of the investigated nuclei [41]. Fig. 3 showed the ^{1}H NMR spectra of DOTAM-*n*-butyl, DOTAM-*n*-butyl-HNO_3 and DOTAM-*n*-butyl-$HReO_4$ in DMSO-d_6. On the basis of the chemical shift and the splitting, the observed chemical shifts were assigned in Table 3. The H(a) atoms can be assigned to N—H group

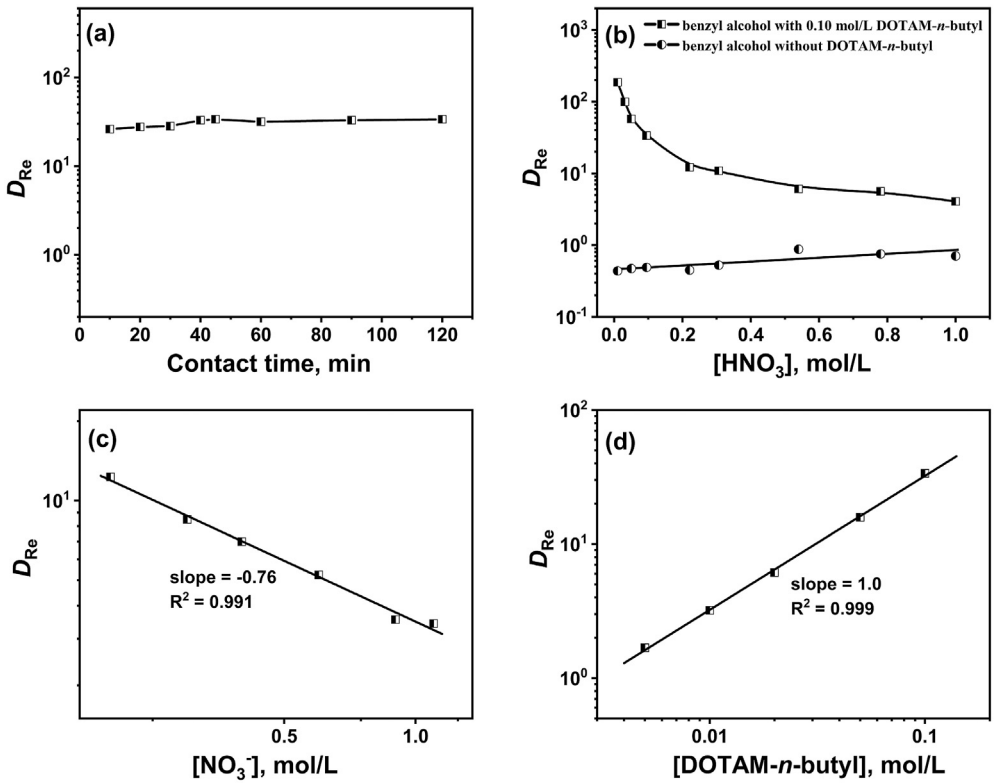

Fig. 2. Distribution ratios of ReO_4^- by DOTAM-*n*-butyl in benzyl alcohol as a function of (a)contact time ([L] = 0.10 mol/L, [ReO_4^-] = 2.7 × 10^{-4} mol/L); (b) HNO_3 concentration ([L] = 0.10 mol/L, [ReO_4^-] = 2.7 × 10^{-4} mol/L); (c) [NO_3^-] concentration ([L] = 0.10 mol/L, [H^+] = 0.10 mol/L, [ReO_4^-] = 2.7 × 10^{-4} mol/L); (d) ligand concentration ([HNO_3] = 0.10 mol/L, [ReO_4^-] = 2.7 × 10^{-4} mol/L).

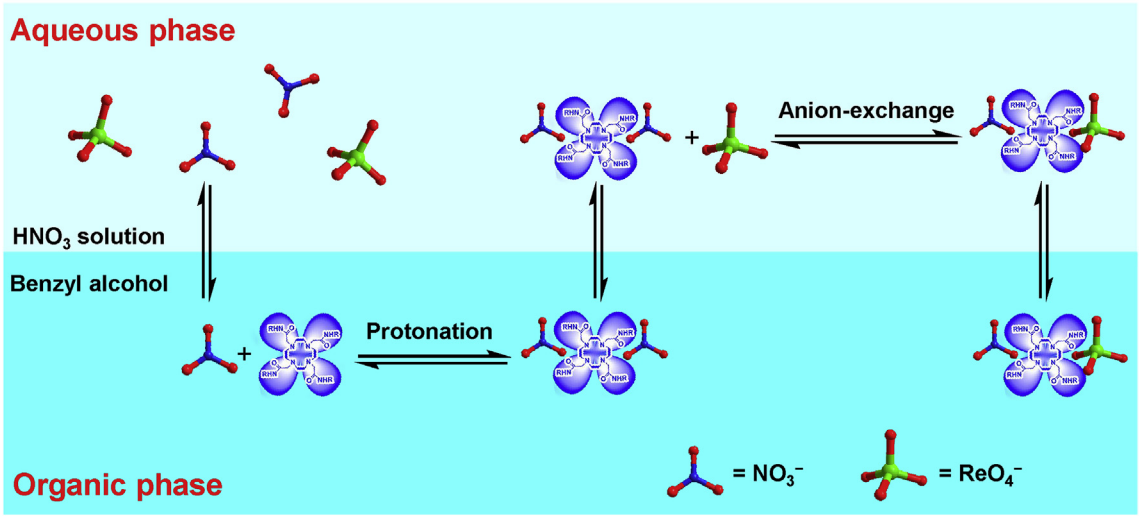

Scheme 2. The extraction process of ReO_4^- in HNO_3 solution by DOTAM-*n*-butyl.

of pendant arm, while H(c) and H(d) atoms belong to the methylene groups next to carbonyl bonds and N atom of amide, respectively. After extracting NO_3^- or ReO_4^-, there was a new resonance band of H(b) at 7.83 ppm in the two complexes, which was attributed to the protonated tertiary amine N—H group of cyclen ring. Meanwhile, Figs. S10 and S12 yet gave the high resolution ESI-MS of DOTAM-*n*-butyl-HNO_3 and DOTAM-*n*-butyl-$HReO_4$. Both of the two highest intensity peaks at *m*/*z* 313.2558 for the former and 313.2586 for the latter originated from the diprotonated molecular species of H_2DOTAM-*n*-butyl^{2+}. Thus, a conclusion can be drawn from these results that a diprotonated species H_2DOTAM-*n*-butyl^{2+} was formed by a reaction of tertiary amine N atoms of cyclen ring with H^+ in the extraction process. Moreover, after extracting NO_3^- or ReO_4^-, the resonance bands of H(a) largely shifted from 7.89 ppm to lower magnetic field by 0.31 and 0.29 ppm, respectively. Whilst the chemical shift of H(c) and H(d) of the two complexes were identical with each other, increasing 0.51 and 0.13 ppm respectively. This is due to the fact that the protonation of N atoms of cyclen ring in

Table 2
The distribution ratios and the separation factors of ReO_4^- over the other anions at various acidity. Organic phase: 0.10 mol/L DOTAM-*n*-butyl in benzyl alcohol; Aqueous phase: 3.0×10^{-4} mol/L of each anions in HNO_3 solution.

Anion	ΔG_h°[a], kJ/mol	Volume[a], Å^3	0.01 mol/L HNO_3		0.05 mol/L HNO_3		0.10 mol/L HNO_3	
			D_A	$SF_{Re/A}$	D_A	$SF_{Re/A}$	D_A	$SF_{Re/A}$
Cl^-	−347	24.8	3.0	27	3.1	9.4	1.4	14
$H_2PO_4^-$	−465	33.5	0.94	86	1.9	15	2.1	9.0
SO_4^{2-}	−1090	51.0	3.0	27	0.80	36	0.68	28
ReO_4^-	−330	73.6	73	–	29	–	19	–

[a] These data were obtained from the literature [39,40].

DOTAM-*n*-butyl leads to a deshielding of the adjacent −CH_2 and −NH groups, and gives rise to a shift of the protons of H(a), H(c) and H(d) to a lower field.

3.2.2. FTIR spectra analysis

For better understanding the complexation of DOTAM-*n*-butyl with ReO_4^-, the FTIR spectra analyses of DOTAM-*n*-butyl, DOTAM-*n*-butyl-HNO_3 and DOTAM-*n*-butyl-$HReO_4$ were also performed. As shown in Fig. 4, with respect to the DOTAM-*n*-butyl FTIR spectrum, the vibrational band at 3200−3400 cm^{-1} and 1659 cm^{-1} could be assigned to the stretching vibrations of N−H and C=O groups, respectively. Both of them also existed in the FTIR spectra of DOTAM-*n*-butyl-HNO_3 and DOTAM-*n*-butyl-$HReO_4$. Nevertheless, the vibrational band at 1659 cm^{-1} translated into a split carbonyl band at 1682 and 1648 cm^{-1} for the former and at 1683 and 1647 cm^{-1} for the latter, separately. The main reason may be that these C=O groups were involved in the different hydrogen bonding interactions and showed the different bond distances in their crystal structures (Tables S3 and S5) [42]. Besides, the two obvious new bands appeared at 1384 and 917 cm^{-1} in the FTIR spectra of DOTAM-*n*-butyl-HNO_3 and DOTAM-*n*-butyl-$HReO_4$, assigned to the asymmetric stretching vibration of NO_3^- and ReO_4^-, respectively. The slightly higher wavenumber in DOTAM-*n*-butyl-$HReO_4$ may be arisen from the intermolecular interactions between ReO_4^- and protonated DOTAM-*n*-butyl. Remarkably, during the preparation process of DOTAM-*n*-butyl-$HReO_4$ complex, the ReO_4^- concentration was equal to that of NO_3^-. However, in the FTIR spectrum of DOTAM-*n*-butyl-$HReO_4$, no characteristic absorption peak of NO_3^- appeared obviously, suggesting that the ReO_4^- had a stronger affinity for protonated DOTAM-*n*-butyl than NO_3^-.

Table 3
The chemical shifts of the ^{1}H NMR spectra of the samples in Fig. 3.

Samples	Chemical shifts (ppm)			
	H(a)	H(b)	H(c)	H(d)
DOTAM-*n*-butyl	7.89	–	3.06	2.95
DOTAM-*n*-butyl-HNO_3	8.20	7.83	3.57	3.08
DOTAM-*n*-butyl-$HReO_4$	8.18	7.83	3.57	3.08

3.2.3. Single crystal X-ray diffraction analysis

Single crystal X-ray diffraction can provide detailed structural information as an essential prerequisite to gain a fundamental understanding of structure property relationships. So the single crystals of the ligand, HNO_3 complex and $HReO_4$ complex were cultivated and analyzed.

The crystal structures of the ligand DOTAM-*n*-butyl and its nitric acid complex DOTAM-*n*-butyl-HNO_3 were shown in Fig. 5. It can be seen that the ligand and HNO_3 complex crystallized in the monoclinic space group of $P2_1/c$ with isostructure. Therein, DOTAM-*n*-butyl possed a centrosymmetric structure with S_2 symmetry, having two pairs of equivalent opposite pendant arms (Fig. 5a). One pair of arms (i.e. one above and the other below the cyclen ring) was further connected to the cyclen ring through intramolecular hydrogen bonds. Whilst the other pair of arms extending and

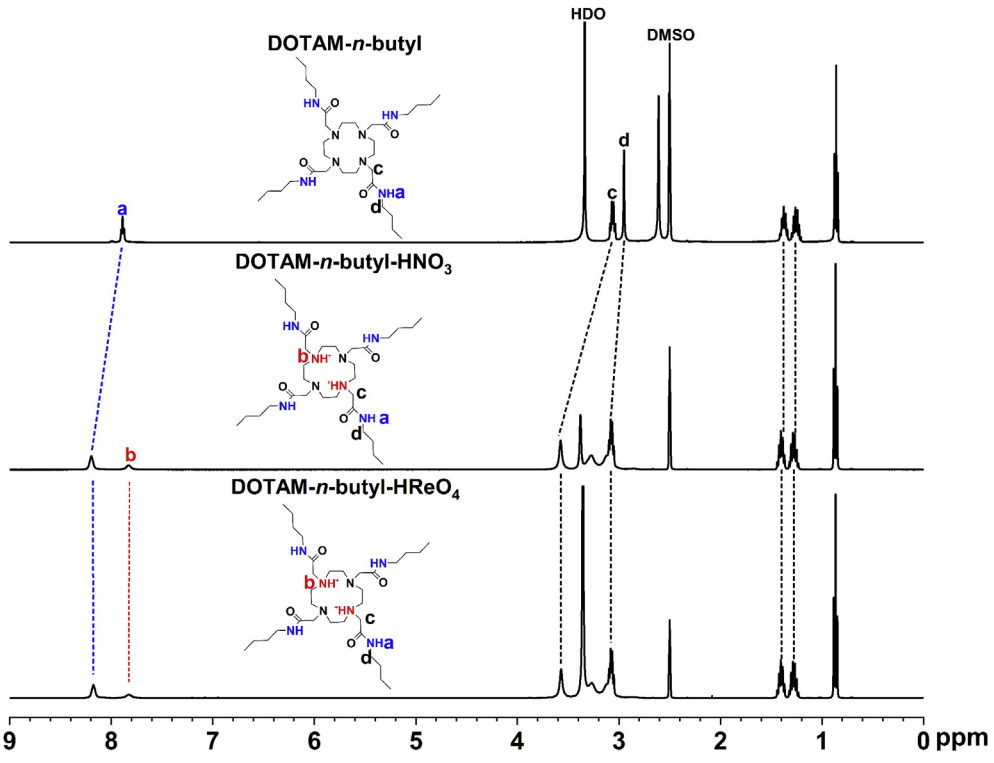

Fig. 3. ^{1}H NMR spectra for DOTAM-*n*-butyl, DOTAM-*n*-butyl-HNO_3 and DOTAM-*n*-butyl-$HReO_4$ in DMSO-d_6.

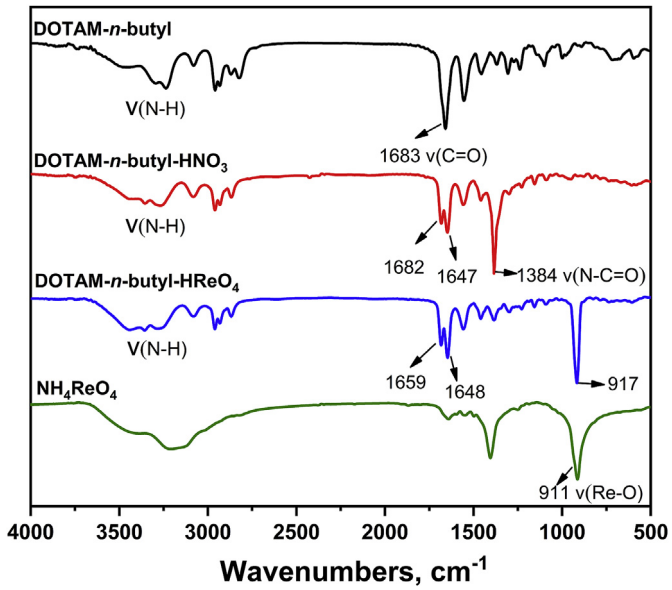

Fig. 4. FT-IR spectra for DOTAM-*n*-butyl, DOTAM-*n*-butyl-HNO_3 and DOTAM-*n*-butyl-$HReO_4$.

pointing away from the cyclen ring was also involved in intermolecular hydrogen bonds (Fig. 5b and Table S2). However, in the crystal structure of DOTAM-*n*-butyl-HNO_3 (Fig. 5c), all four arms were extended to one side of the cyclen ring plane and two trans-disposed N atoms of cyclen ring were protonated to form a cation of H_2DOTAM-*n*-butyl^{2+}. A 1:2 association complex (H_2DOTAM-*n*-butyl$^{2+}\cdot 2NO_3^-$) was generated by means of an electrostatic interaction with two counterions of NO_3^-, which was also in agreement with the above result of HNO_3 extraction. Meanwhile, it was also observed a bilayer structure with an ABAB stacking mode in the crystal of DOTAM-*n*-butyl-HNO_3 (Fig. 5d), which NO_3^- ions were located in the gap between the upper and lower structural layers. There were also multiple hydrogen bond interactions between NO_3^- ions and H_2DOTAM-*n*-butyl^{2+} (Table S5).

As far as the $HReO_4$ complexes be concerned, only the single crystal of DOTAM-benzyl-$HReO_4$ was acquired. Great efforts were also made to obtain the single crystal of DOTAM-*n*-butyl-$HReO_4$ complex. Unfortunately, although fast and careful handling of the crystals during the measurement, the crystal structure suffered from a significant decrease in quality since the carbon chains of side arms were disordered by interacting on each other and the highest residual electron density peaks were located near the Re atoms, reflected in a number of corresponding A and B level alerts in the checkcif report (CCDC 1505095). Despite all this, it can still be seen clearly that two ReO_4^- ions have electrostatic interactions with one diprotonated H_2DOTAM-*n*-butyl^{2+} cation (Fig. S16). The crystal structure of DOTAM-benzyl-$HReO_4$ was shown in Fig. 6. It was clear that two trans-disposed nitrogens of cyclen ring were protonated, and four arms all were extended to one side of cyclen ring plane to compatible with the tetrahedral ReO_4^- ion (Fig. 6a). Similar to the structure of DOTAM-*n*-butyl-HNO_3, there was also an ABAB bilayer structure in that of DOTAM-benzyl-$HReO_4$ (Fig. 6d). And the ReO_4^- ions also resided in the gap between the upper and lower layers, having multiple hydrogen bonding interactions with N—H groups and C—H groups of pendant arms, and C—H groups of cyclen rings (Fig. 6b and d). The related bond distances and angles of hydrogen bonds were listed in Table S6. The space-filling models further revealed that the interlayer gap was compatible with the tetrahedral ReO_4^- ion (Fig. 6c). As a result, it could be deduced that the

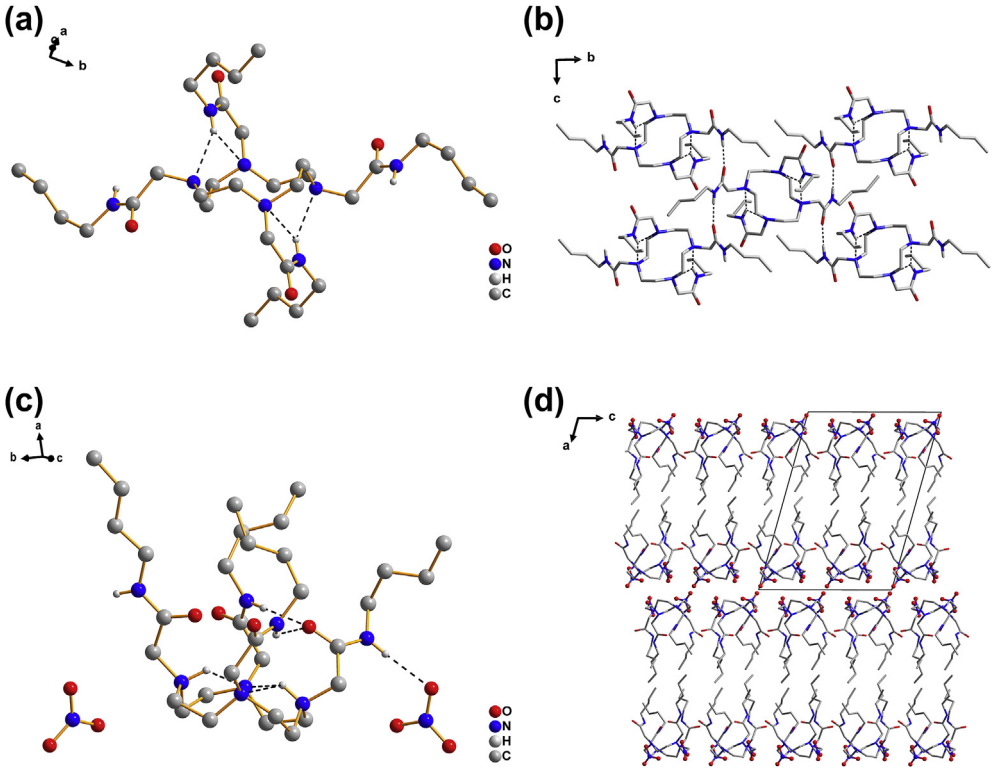

Fig. 5. Crystal structures of DOTAM-*n*-butyl and DOTAM-*n*-butyl-HNO_3: (a) asymmetric unit of DOTAM-*n*-butyl (the black dotted lines represent hydrogen bonds); (b) the intermolecular hydrogen bonding interactions of the amide groups in DOTAM-*n*-butyl; (c) asymmetric unit of DOTAM-*n*-butyl-HNO_3; (d) layer structure of H_2DOTAM-*n*-butyl-HNO_3 viewed along the *b* axis. Hydrogen atoms are omitted for clarity. Nonrelevant hydrogen atoms are omitted for clarity.

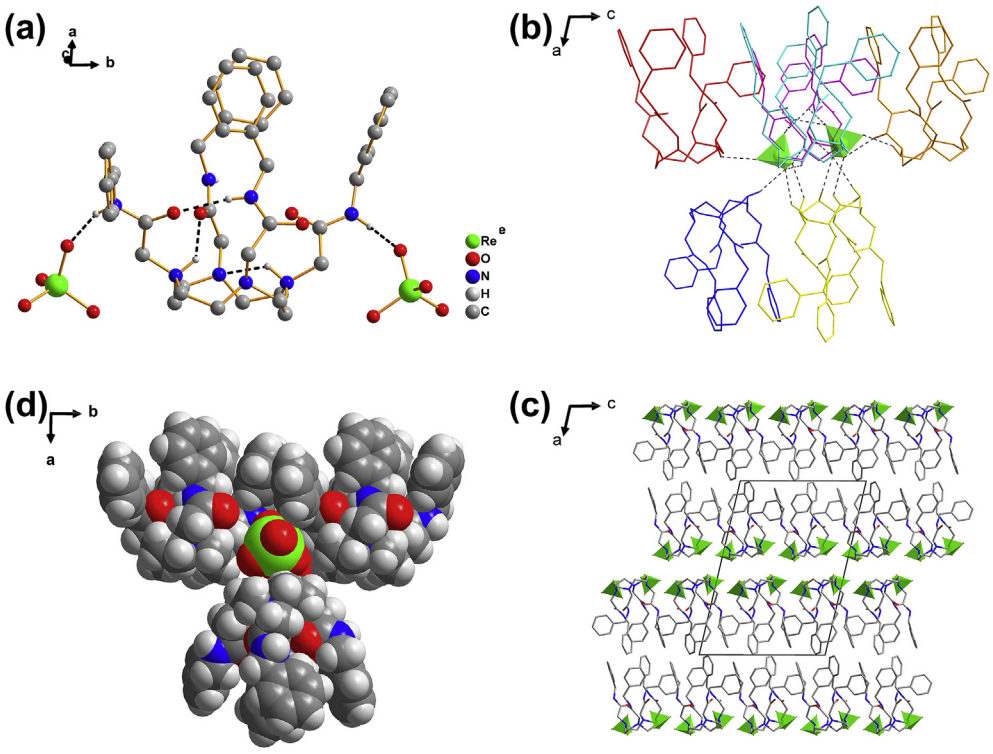

Fig. 6. Crystal structures of DOTAM-benzyl-$HReO_4$: (a) asymmetric unit of DOTAM-benzyl-$HReO_4$ (the black dotted lines represent hydrogen bonds); (b) hydrogen bonds formed between ReO_4^- and six H_2DOTAM-benzyl^{2+} (the green polyhedrons represent ReO_4^- ions and six H_2DOTAM-benzyl^{2+} are shown in different colors); (c) a space-filling model of ReO_4^- and six H_2DOTAM-benzyl^{2+}; (d) layer structure of DOTAM-benzyl-$HReO_4$ viewed along the *b* axis. Hydrogen atoms are omitted for clarity.

extraction of ReO_4^- was an ion-pair extraction through electrostatic interactions as well as hydrogen bonding interactions.

Table S6

However, 1:2 complex of the ligand with ReO_4^- in crystal structure was not consistent with the extraction result of 1:1 complex in solution. It is not strange at all. This difference was a common phenomenon in the research of solvent extraction and might be attributed to their fully different coordinated environments [43–46]. Besides, the type of complex formed was also depended on the concentration of ligand and cation or anion [43–45]. For example, Drew et al. investigated a series of 1:1 complexes of terpyridine ligand with the lanthanides and found that it was more likely to form the complexes with 1:2 metal to ligand ratio for heavier lanthanides with increasing the terpyridine concentration [43]. In solvent extraction experiments, the concentration of DOTAM-*n*-butyl was much more than that of ReO_4^- (over 300 times), whilst ReO_4^- concentration was only twice as that of the ligand during the preparation process of ligand-$HReO_4$ complex. The substantial increase of ReO_4^- concentration might be likely to lead to the formation of 1:2 complex of the ligand with ReO_4^-. In the present work, although the results obtained from slope analyses in solvent extraction were inconsistent with those from X-ray diffraction, the studies on crystal structure still have important implications for understanding the interaction between DOTA-tetraamide ligand and ReO_4^- ion in solvent extraction.

4. Conclusions

The two DOTAM-*n*-butyl and DOTAM-benzyl ligands were synthesized for investigating the extraction and complexation behaviors toward ReO_4^- in HNO_3 solution. In acid solution, DOTAM-*n*-butyl was liable to be protonated. The analyses of crystal structure for DOTAM-*n*-butyl-HNO_3 showed the formation of 1:2 complex of DOTAM-*n*-butyl with HNO_3. DOTAM-*n*-butyl exhibited strong extraction ability and good selectivity for ReO_4^-. The slope analyses revealed that 1:1 complex of DOTAM-*n*-butyl with ReO_4^- was generated in solvent extraction processes and ReO_4^- was extracted by means of the substitution of one ReO_4^- for one NO_3^- in the 1:2 complex with HNO_3. The solvent extraction and X-ray crystallography demonstrated an anion-exchange extraction model. X-ray crystal structure analyses of the ligand-$HReO_4$ complex indicated that the ion-pairs were formed through electrostatic interactions and multiple hydrogen bonding interactions between the protonated ligand and ReO_4^- ions. As a whole, this work provided an efficient separation method for ReO_4^- based on DOTA-tetraamide extractant. Although the properties of ReO_4^- are not always the same as those of TcO_4^-, the results of this paper may provide important guidance and reference to design of new and more efficient ligands for TcO_4^- extraction from acid medium in the future.

Declaration of competing interest

The authors declare that they have no known competing financial interests or personal relationships that could have appeared to influence the work reported in this paper.

CRediT authorship contribution statement

Xueyu Wang: Conceptualization, Methodology, Software, Investigation, Validation, Data curation, Writing - review & editing. **Xiaoyang Hu:** Software, Formal analysis, Validation, Resources, Data curation, Writing - original draft. **Lianjun Song:** Resources, Formal analysis, Visualization. **Xiuying Yang:** Writing - review & editing, Supervision, Data curation. **Qian Xiao:** Writing - review & editing, Supervision, Data curation. **Haowei Xu:** Writing - review & editing. **Songdong Ding:** Writing - review & editing, Visualization,

Supervision, Project administration, Funding acquisition.

Acknowledgments

The authors are sincerely grateful for the financial support by the National Natural Science Foundation of China (Grant Nos. 11975161 and 11675115). The comprehensive training platform of specialized laboratory, College of chemistry, Sichuan University is acknowledged for FTIR, NMR, ESI-MS, ICP-AES and X-ray diffraction analyses.

Appendix A. Supplementary data

Supplementary data to this article can be found online at https://doi.org/10.1016/j.molstruc.2020.128330.

References

[1] F.N. Smith, C.D. Taylor, W. Um, A.A. Kruger, Technetium incorporation into goethite (α-FeOOH): an atomic-scale investigation, Environ. Sci. Technol. 49 (2015) 13699–13707.
[2] A.M. Desai, P.K. Singh, An ultrafast molecular-rotor-based fluorescent turn-on sensor for the perrhenate anion in aqueous solution, Chem. Eur J. 25 (2019) 2035–2042.
[3] Y. Gao, C. Chen, H. Chen, R. Zhang, X. Wang, Synthesis of a novel organic-inorganic hybrid of polyaniline/titanium phosphate for Re(VII) removal, Dalton Trans. 44 (2015) 8917–8925.
[4] X. Shu, L. Shen, Y. Wei, D. Hua, Synthesis of surface ion-imprinted magnetic microsphere for efficient sorption of perrhenate: a structural surrogate for pertechnetate, J. Mol. Liq. 211 (2015) 621–627.
[5] M. Chotkowski, D. Połomski, Extraction of pertechnetates from HNO_3 solutions into ionic liquids, J. Radioanal. Nucl. Chem. 314 (2017) 87–92.
[6] D. Banerjee, D. Kim, M.J. Schweiger, A.A. Kruger, P.K. Thallapally, Removal of TcO_4^- ions from solution: materials and future outlook, Chem. Soc. Rev. 45 (2016) 2724–2739.
[7] J. Li, X. Dai, L. Zhu, C. Xu, D. Zhang, M.A. Silver, P. Li, L. Chen, Y. Li, D. Zuo, H. Zhang, C. Xiao, J. Chen, J. Diwu, O.K. Farha, T.E. Albrecht-Schmitt, Z. Chai, S. Wang, $^{99}TcO_4^-$ remediation by a cationic polymeric network, Nat. Commun. 9 (2018) 3007.
[8] D. Banerjee, S.K. Elsaidi, B. Aguila, B. Li, D. Kim, M.J. Schweiger, A.A. Kruger, C.J. Doonan, S. Ma, P.K. Thallapally, Removal of pertechnetate-related oxyanions from solution using functionalized hierarchical porous frameworks, Chem. Eur J. 22 (2016), 17581–17584.
[9] D. Sheng, L. Zhu, C. Xu, C. Xiao, Y. Wang, Y. Wang, L. Chen, J. Diwu, J. Chen, Z. Chai, T.E. Albrecht-Schmitt, S. Wang, Efficient and selective uptake of TcO_4^- by a cationic metal-organic framework material with open Ag^+ sites, Environ. Sci. Technol. 51 (2017) 3471–3479.
[10] G. Tian, P. Zhang, J. Wang, L. Rao, Extraction of actinide(III, IV, V, VI) ions and TcO_4^- by N,N,N′,N′-tetraisobutyl-3-oxa-glutaramide, Solvent Extr, Ion Exch 23 (2005) 631–643.
[11] A.B. Melent'ev, A.N. Mashkin, O.V. Tugarina, D.N. Kolupaev, B.Y. Zilberman, I.G. Tananaev, Effect of some reducing and complexing agents on the extraction behavior of technetium in the TBP-HNO_3 system, Radiochemistry 53 (2011) 256–263.
[12] F. El Kalai, T. Chelfi, N. Benchat, B. Hacht, M. Bouklah, A. Elaatiaoui, S. Daoui, M. Allali, T. Ben Hadda, F. Almalki, New organic extractant based on pyridazinone scaffold compounds: liquid-liquid extraction study and DFT calculations, J. Mol. Struct. 1191 (2019) 24–31.
[13] I. Kumari, B.V.R. Kumar, A. Khanna, A review on UREX processes for nuclear spent fuel reprocessing, Nucl. Eng. Des. 358 (2020) 110410.
[14] A.M. Ngcephe, M.K. Sinha, W. Purcell, Solvent extraction and separation of palladium from platinum group elements: synthesis and characterization of 2-mercaptopyridine N-oxide-palladium (II) complex, J. Mol. Struct. 1199 (2020) 127009.
[15] V. Mikulaj, F. Macášek, P. Rajec, Simultaneous extraction of palladium and technetium from nitrate solutions with tri-n-octylamine, J. Radioanal. Nucl. Chem. 51 (1979) 55–62.
[16] A. ElKot, Solvent extraction of heptavalent technetium, J. Radioanal. Nucl. Chem. 163 (1992) 363–372.
[17] K.M. Rohal, D.M.V. Seggen, J.F. Clark, M.K. McClure, C. Kevin Chambliss, S.H. Strauss, N.C. Schroeder, Solvent extraction of pertechnetate and perrhenate ions from nitrate-rich acidic and alkaline aqueous solutions, Solvent Extr. Ion Exch. 14 (1996) 401–416.
[18] A. Landgren, J.O. Liljenzin, Extraction behaviour of technetium and actinides in the Aliquat-336/nitric acid system, Solvent Extr. Ion Exch. 17 (1999) 1387–1401.
[19] Y. Bal, K.E. Bal, G. Cote, A. Lallam, Characterization of the solid third phases that precipitate from the organic solutions of Aliquat-336 after extraction of molybdenum(VI) and vanadium(V), Hydrometallurgy 75 (2004) 123–134.
[20] E.A. Katayev, Y.A. Ustynyuk, J.L. Sessler, Receptors for tetrahedral oxyanions, Coord. Chem. Rev. 250 (2006) 3004–3037.
[21] K. Wichmann, B. Antonioli, T. Söhnel, M. Wenzel, K. Gloe, K. Gloe, J.R. Price, L.F. Lindoy, A.J. Blake, M. Schröder, Polyamine-based anion receptors: extraction and structural studies, Coord. Chem. Rev. 250 (2006) 2987–3003.
[22] E.A. Katayev, G.V. Kolesnikov, J.L. Sessler, Molecular recognition of pertechnetate and perrhenate, Chem. Soc. Rev. 38 (2009) 1572–1586.
[23] R. Alberto, G. Bergamaschi, H. Braband, T. Fox, V. Amendola, $^{99}TcO_4^-$: selective recognition and trapping in aqueous solution, Angew. Chem. Int. Ed. 51 (2012) 9772–9776.
[24] V. Amendola, G. Bergamaschi, M. Boiocchi, R. Alberto, H. Braband, Fluorescent sensing of ^{99}Tc pertechnetate in water, Chem. Sci. 5 (2014) 1820–1826.
[25] H.M.Y. Tsukube, S. Shinoda, M. Tadokoro, K. Hori, Na^+ ion-specific binding and extraction by lipophilic armed cyclens via octadentate encapsulation, Tetrahedron Lett. 38 (1997) 5021–5024.
[26] H.M.Y. Tsukube, S. Shinoda, T. Okazaki, M. Tadokoro, K. Hori, Side arm effects on cyclen–alkali metal cation complexation: highly selective and three-dimensional encapsulation of Na^+ ion, Inorg. Chem. 38 (1999) 3506–3512.
[27] A. Bianchi, L. Calabi, C. Giorgi, P. Losi, P. Mariani, P. Paoli, P. Rossi, B. Valtancoli, M. Virtuani, Thermodynamic and structural properties of Gd^{3+} complexes with functionalized macrocyclic ligands based upon 1,4,7,10-tetraazacyclododecane, J. Chem. Soc., Dalton Trans. (2000) 697–705.
[28] F. Cuenot, M. Meyer, E. Espinosa, A. Bucaille, R. Burgat, R. Guilard, C. Marichal-Westrich, New insights into the complexation of Lead(II) by 1,4,7,10-tetrakis(carbamoylmethyl)-1,4,7,10-tetraazacyclododecane (DOTAM): structural, thermodynamic, and kinetic studies, Eur. J. Inorg. Chem. (2008) 267–283.
[29] T. Mani, G. Tircso, P. Zhao, A.D. Sherry, M. Woods, Effect of the regiochemistry of butyl amide substituents on the solution-state structures of lanthanide(III) DOTA-tetraamide complexes, Inorg. Chem. 48 (2009) 10338–10345.
[30] Q. Deng, Y. Jin, Q. Wang, R. Zhao, N. Pan, F. Zhai, M. Luo, C. Xia, New cyclen derivative ligand for thorium(IV) separation by solvent extraction, J. Radioanal. Nucl. Chem. 295 (2013) 125–133.
[31] S.E. Pepper, M.D. Ogden, Perrhenate extraction studies by Cyphos 101-IL; screening for implementation in technetium removal, Separ. Purif. Technol. 118 (2013) 847–852.
[32] G. Zucchi, R. Scopelliti, P.-A. Pittet, J.C.G. Bünzli, R.D. Rogers, Structural and photophysical behaviour of lanthanide complexes with a tetraazacyclododecane featuring carbamoyl pendant arms, J. Chem. Soc., Dalton Trans. (1999) 931–938.
[33] T. Mani, G. Tircso, P. Zhao, A.D. Sherry, M. Woods, Effect of the regiochemistry of butyl amide substituents on the solution-state structures of lanthanide(III) DOTA-tetraamide complexes, Inorg. Chem. 48 (2009) 10338–10345.
[34] O.V. Dolomanov, L.J. Bourhis, R.J. Gildea, J.A.K. Howard, H. Puschmann, OLEX2: a complete structure solution, refinement and analysis program, J. Appl. Crystallogr. 42 (2009) 339–341.
[35] G.M. Sheldrick, SHELXT-integrated space-group and crystal-structure determination, Acta Crystallogr. A: Found. of Crystallogr. 71 (2015) 3–8.
[36] G.M. Sheldrick, Crystal structure refinement with SHELXL, Acta Crystallogr. C: Struct. Chem. 71 (2015) 3–8.
[37] S. StenstrSm, G. Aly, Extraction of cadmium from phosphoric acid solutions with amines. Part II. Diluent selection, flow-sheet configuration, pilot plant operation, Hydrometallurgy 14 (1985) 257–276.
[38] K. Nazari, A. Ghadiri, H. Babaie, Elimination of cadmium from wet process phosphoric acid with Alamine 336, Miner. Eng. 18 (2005) 1233–1238.
[39] Y. Marcus, H. Donald Brooke Jenkins, L. Glasser, Ion volumes: a comparison, J. Chem. Soc., Dalton Trans. (2002) 3795–3798.
[40] R. Custelcean, B.A. Moyer, Anion separation with metal-organic frameworks, Eur. J. Inorg. Chem. (2007) 1321–1340.
[41] G. Kapur, A. Ecker, R. Meusinger, Establishing quantitative structure-property relationships (QSPR) of diesel samples by proton-NMR & multiple linear regression (MLR) analysis, Energy Fuel. 15 (2001) 943–948.
[42] F. Cuenot, M. Meyer, E. Espinosa, R. Guilard, Synthesis, characterization, and X-ray crystal structures of cyclam derivatives. 8. Thermodynamic and kinetic appraisal of Lead (II) chelation by octadentate carbamoyl-armed macrocycles1, Inorg. Chem. 44 (2005), 7895–7910.
[43] M.G.B. Drew, P.B. Iveson, M.J. Hudson, J.O. Liljenzin, L. Spjuth, P.-Y. Cordier, Å. Enarsson, C. Hill, C. Madic, Separation of americium(III) from europium(III) with tridentate heterocyclic nitrogen ligands and crystallographic studies of complexes formed by 2,2′:6′,2″-terpyridine with the lanthanides, J. Chem. Soc., Dalton Trans. (2000) 821–830.
[44] D.G.K. Farrell, K. Gloe, G. Goretzki, V. McKee, J. Nelson, M. Nieuwenhuyzen, I. Pál, H. Stephan, R.M. Town, K. Wichmann, Towards promising oxoanion extractants: azacages and open-chain counterparts, Dalton Trans. (2003) 1961–1968.
[45] M.R.S. Foreman, M.J. Hudson, M.G.B. Drew, C. Hill, C. Madic, Complexes formed between the quadridentate, heterocyclic molecules 6,6′-bis-(5,6-dialkyl-1,2,4-triazin-3-yl)-2,2′-bipyridine (BTBP) and lanthanides(III): implications for the partitioning of actinides(III) and lanthanides(III), Dalton Trans. (2006) 1645–1653.
[46] M. Nilsson, S. Andersson, F. Drouet, C. Ekberg, M. Foreman, M. Hudson, J.O. Liljenzin, D. Magnusson, G. Skarnemark, Extraction properties of 6,6′-Bis-(5,6-dipentyl-[1,2,4]triazin-3-yl)-[2,2′]bipyridinyl (C5-BTBP), Solvent Extr, Ion Exch 24 (2006) 299–318.